Journal of Sound and Vibration 330 (2011) 615–624

Contents lists available at ScienceDirect

Journal of Sound and Vibration

journal homepage: www.elsevier.com/locate/jsvi

# Active control of sound radiated by a submarine in bending vibration

Mauro Caresta *

*School of Mechanical and Manufacturing Engineering, The University of New South Wales, Sydney, 2052 NSW, Australia*

ARTICLE INFO

*Article history:*
Received 25 May 2010
Received in revised form
10 August 2010
Accepted 5 September 2010
Handling Editor: L.G. Tham
Available online 28 September 2010

ABSTRACT

This paper theoretically investigates the use of inertial actuators to reduce the sound radiated by a submarine hull in bending vibration under harmonic excitation from the propeller. The radial forces from the propeller are tonal at the blade passing frequency and are transmitted to the hull through the stern end cone. The hull is modelled as a fluid loaded cylindrical shell with ring stiffeners and two equally spaced bulkheads. The cylinder is closed by end-plates and conical end caps. The actuators are arranged in circumferential arrays and attached to the prow end cone. Both Active Vibration Control and Active Structural Acoustic Control are analysed. The inertial actuators can provide control forces with a magnitude large enough to reduce the sound radiated by the vibrations of the hull in some frequency ranges.

© 2010 Elsevier Ltd. All rights reserved.

## 1. Introduction

Active control techniques to reduce both the vibrations and the sound radiated by flexible structures have received much attention in the past three decades. Two main strategies have been developed: the Active Vibration Control (AVC) focused on reducing the vibration level of the structure, and the Active Structural Acoustic Control (ASAC) aimed to reduce the structure-born sound by application of secondary forces [1]. Active Control is now well established and successfully applied to many engineering applications as a valid alternative to passive control techniques, especially in the low frequency range. Low frequency radiated noise is an important issue in ships and submarines due to the fluctuating forces from the propeller at the blade passing frequency (rotational speed of the shaft multiplied by the number of blades on the propeller). The harmonic forces result from the rotation of the propeller in a spatially non-uniform wake [2]. Due to the size of marine vessels and the magnitude of the forces involved, only passive control techniques applied to the propeller shafting system [3,4] or modification to the propeller and thrust bearing [5,6] seems to be practical. More work is then needed in order to apply active control strategies to such large structures. Recently Pan et al. [7,8] presented active control of the low frequency radiated noise for a submarine hull, in which the control moment was generated on the ring stiffener of the hull. In this work, active control techniques are investigated to reduce the low frequency sound radiated by a large submarine hull under radial excitation from the propeller. Inertial actuators are arranged in circumferential arrays and positioned on the prow end conical shell in order to produce secondary forces to reduce the primary effect of the propeller force. The performances of both AVC and ASAC are analysed. The quadratic optimisation theory is used to calculate the control forces. The optimisation is aimed to minimise a cost function based on the structural response (AVC) or the acoustic response (ASAC) at some locations using sensors error. In particular the ASAC implies the use of microphones but in many applications this cannot be done into operating conditions. Some researchers have then investigated the use of error sensors located directly on the structure to estimate the far-field sound pressure. Baumann et al. [9] proposed the use of

* Tel.: +61 293 854 763; fax: +61 296 631 222.
*E-mail address:* mcaresta@yahoo.it

0022-460X/$ - see front matter © 2010 Elsevier Ltd. All rights reserved.
doi:10.1016/j.jsv.2010.09.006

radiation filters to estimate the radiated sound power from measurements on a clamped–clamped beam. Polyvinylidene fluoride sensors were used to observe the vibration modes with higher radiation efficiency [10,11]. Maillard and Fuller [12] investigated the use of piezoelectric actuators to reduce the sound radiated by a cylinder using point sensors on the structure to estimate the radiated pressure. This technique known as Discrete Structural Acoustic Sensing (DSAS) and originally applied to planar radiators [13], consists in using arrays of structural sensors whose output is filtered to estimate the far-field sound pressure with the Helmholtz integral formulation. In the aforementioned works much effort was put on building a function to estimate the far-field sound pressure by several measurements on the structure.

In this work the sound radiated by the submarine hull in the far field, is divided in the frequency domain by the axial displacement of the hull in order to define an acoustic transfer function. The transfer function is calculated numerically but in a real structure it can be estimated just once before it becomes operative. Once the transfer function is known in the frequency domain, it can be implemented to filter the measurement of the axial displacement and estimate the radiated sound pressure at different far-field locations. Only one point measurement on the structure is needed.

## 2. Structural model of the submarine hull

A detailed semi-analytical model to study the dynamical and acoustic behaviour of a submarine hull under asymmetric excitation was presented by Caresta and Kessissoglou [14] and is briefly reported here for completeness. The submarine hull is modelled as ring stiffened cylindrical shell with two equally spaced bulkheads and closed by two truncated conical shells as shown in Fig. 1. Fluid loading from the external water is taken into account.

### 2.1. Model of the fluid loaded cylindrical and conical shells

The cylindrical shell of thickness $h$ is modelled using the Flügge thin shell theory and the dynamic effect of the ring stiffened is taken into account averaging the stiffener properties on the shell [15]. The equations of motion are given in terms of $u$, $v$ and $w$ that are the axial, circumferential and radial components of the shell displacement, respectively, as function of the axial coordinate $x$ and the angle $\theta$ as shown in Fig. 2.

A time dependence of the kind $e^{-j\omega t}$ is considered in this work and it is omitted in the equations, $\omega$ is the circular frequency. The equations of motion for the vibrations of the stiffened fluid loaded shell are given by [14]:

$$L_{11}u+L_{12}v-L_{13}w=-\gamma\rho h\omega^2 u \tag{1}$$

$$L_{21}u+L_{22}v-L_{23}w=-\gamma\rho h\omega^2 v \tag{2}$$

$$L_{31}u+L_{32}v-L_{33}w-p=-\gamma\rho h\omega^2 w \tag{3}$$

$\rho$ is the material density, $p$ is the external pressure from the water, $c_L$ is the longitudinal wave speed, the coefficient $\gamma$ takes into account the increase of inertia given by the stiffener and the distributed mass and can be found in Ref. [14] together with the partial differential operators $L_{ij}$. The displacement components for the cylindrical shell can, respectively, be

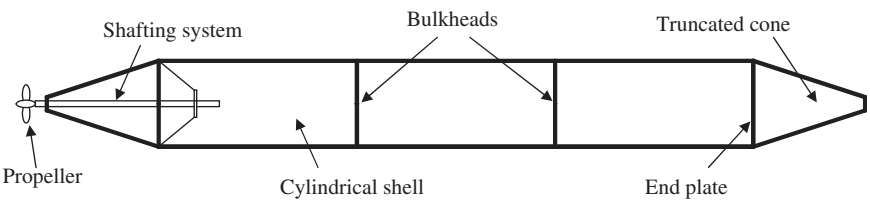


**Fig. 1.** Model of the submerged vessel.

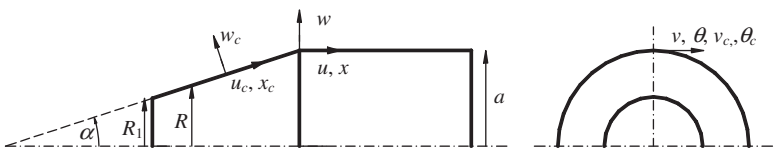


**Fig. 2.** Displacements for the joined conical–cylindrical shell.

written in form of wave propagation as

$$u(x,\theta)=\sum_{n=0}^{\infty}\sum_{i=1}^{8}C_{n,i}W_{n,i}e^{jk_{n,i}x}\cos(n\theta) \tag{4}$$

$$v(x,\theta)=\sum_{n=0}^{\infty}\sum_{i=1}^{8}G_{n,i}W_{n,i}e^{jk_{n,i}x}\sin(n\theta) \tag{5}$$

$$w(x,\theta)=\sum_{n=0}^{\infty}\sum_{i=1}^{8}W_{n,i}e^{jk_{n,i}x}\cos(n\theta) \tag{6}$$

$C_{n,i}=U_{n,i}/W_{n,i}$ and $G_{n,i}=V_{n,i}/W_{n,i}$ are the amplitude ratio and $U_{n,i}$, $V_{n,i}$, $W_{n,i}$ are the wave amplitude coefficients of the displacement. The equations of motion for a truncated cone of semi-vertex angle $\alpha$ are given in terms of $u_c$, $v_c$ and $w_c$, which are, respectively, the orthogonal components of the displacement in the $x_c$, $\theta_c$ and radial directions as shown in Fig. 2. The equations of motion to describe the dynamic responses of a fluid loaded conical shell are given by

$$L_{c,11}u_c+L_{c,12}v_c-L_{c,13}w_c=-\rho h_c\omega^2u_c \tag{7}$$

$$L_{c,21}u_c+L_{c,22}v_c-L_{c,23}w_c=-\rho h_c\omega^2v_c \tag{8}$$

$$L_{c,31}u_c+L_{c,32}v_c-L_{c,33}w_c-p_c=-\rho h_c\omega^2w_c \tag{9}$$

$h_c$ is thickness of the conical shell, the external pressure $p_c$ and the partial differential operators $L_{c,ij}$ can be found in [14]. Expanding the displacements with power series and substituting them on the equations of motion, the solutions take the following form:

$$u_c(x_c,\theta_c)=\sum_{n=0}^{\infty}\mathbf{u}_{c,n}\cdot\mathbf{x}_{c,n}\cos(n\theta_c) \tag{10}$$

$$v_c(x_c,\theta_c)=\sum_{n=0}^{\infty}\mathbf{v}_{c,n}\cdot\mathbf{x}_{c,n}\sin(n\theta_c) \tag{11}$$

$$w(x_c,\theta_c)_c=\sum_{n=0}^{\infty}\mathbf{w}_{c,n}\cdot\mathbf{x}_{c,n}\cos(n\theta_c) \tag{12}$$

$\mathbf{x}_{c,n}$ is the vector of the eight unknown coefficients

$$\mathbf{x}_{c,n}=\begin{bmatrix}a_{0,n} & a_{1,n} & b_{0,n} & b_{1,n} & c_{0,n} & c_{1,n} & c_{2,n} & c_{3,n}\end{bmatrix}^T \tag{13}$$

$\boldsymbol{u}_{c,n}$, $\boldsymbol{v}_{c,n}$, $\boldsymbol{w}_{c,n}$ can be found in [14]. The cylindrical and the conical shells can be coupled together by applying the continuity conditions at the junction [16].

### 2.2. Model of the bulkheads

The bulkheads and the end-plates are modelled as thin circular plates of thickness $h$. The equations of motion for the axial $w_p$, circumferential $v_p$ and radial $u_p$ components of the displacement are given in polar coordinates $(r, \theta_p)$ [17]:

$$L_{p,33}w_p=-\omega^2w_p \tag{14}$$

$$L_{p,11}u_p+L_{p,12}v_p=-\omega^2v_p \tag{15}$$

$$L_{p,21}u_p+L_{p,22}v_p=-\omega^2u_p \tag{16}$$

The solutions of the equations are given in terms of Bessel functions [17,18]:

$$w_p(r,\theta_p)=\sum_{n=0}^{\infty}(A_{n,1}J_n(k_{pB}r)+A_{n,2}I_n(k_{pB}r))\cos(n\theta_p) \tag{17}$$

$$v_p(r,\theta_p)=-\sum_{n=0}^{\infty}\left(\frac{nB_{n,1}J_n(k_{pL}r)}{r}+B_{n,2}\frac{\partial J_n(k_{pT}r)}{\partial r}\right)\sin(n\theta_p) \tag{18}$$

$$u_p(r,\theta_p)=\sum_{n=0}^{\infty}\left(B_{n,1}\frac{\partial J_n(k_{pL}r)}{\partial r}+\frac{nB_{n,2}J_n(k_{pT}r)}{r}\right)\cos(n\theta_p) \tag{19}$$

$D=Eh_p^3(12-\upsilon^2)$ is the flexural rigidity, $k_{pB}=(\rho\omega^2 h_p/D)^{1/4}$ is the plate bending wavenumber and $k_{pL}=\omega[\rho(1-\upsilon^2)/E]^{1/2}$ is the wavenumber for longitudinal in-plane waves. $E$, $\rho$ and $\upsilon$ are Young's modulus, density and Poisson's ratio of the material. The coefficients $A_{n,i}$ and $B_{n,i}$ $(i=1,2)$ are determined from the boundary conditions. The displacements for both the cylindrical shell, the cones and the circular plates are written as an infinite summation of circumferential harmonics of order $n$. $n=0$ results in an axisymmetric vibration, the bending modes happen with $n=1$ and are the primary concern of this paper.

### 2.3. Excitation from the propeller

Rotation of the propeller through a non-uniform wake results in fluctuating forces in both axial and radial directions [20]. The aim of this study is to investigate the reduction of the sound radiated by the vibrations induced by the radial component of the harmonic forces. The dynamics of the propeller-shafting system mainly affect the axial motion of the hull and can be neglected to study the bending behaviour of the submarine hull. The radial component of the force can be approximated as a point force applied to the extremity of the end cone as shown in Fig. 3, exciting all circumferential order

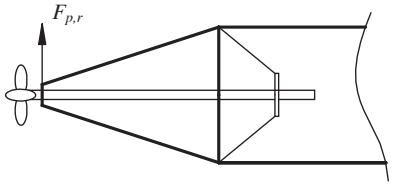


**Fig. 3.** Radial component of the fluctuating propeller force.

modes. A point force located on the shell at $(x_0, \theta_0)$ can be described in terms of the Dirac delta as function of the arc length $\sigma=r_0\theta$, with $r_0$ the shell radius

$$F(x_0,\sigma_0)=F_0\delta(\sigma-\sigma_0)e^{-j\omega t} \tag{20}$$

where the delta function $\delta(\sigma-\sigma_0)$ has the dimension of $(\mathrm{m}^{-1})$. With $T_{x_0}=2\pi r_0$, the delta function $\delta(\sigma-\sigma_0)$ can be expanded as a Fourier series around the circumference as

$$\delta(\sigma-\sigma_0)=\frac{1}{T_{x_0}}+\frac{2}{T_{x_0}}\sum_{n=1}^{\infty}\cos\left(\frac{2\pi n\sigma}{T_{x_0}}\right) \tag{21}$$

### 2.4. Boundary and continuity conditions

The dynamic response of the entire submarine structure for every circumferential mode number $n$ is expressed in terms of $W_{n,i}$ $(i=1{:}8)$ for each section of the hull, $A_{n,i}$, $B_{n,i}$ $(i=1,\ 2)$ for each circular plate, and $\mathbf{x}_{c,n}$ for each piece of frustum of cone. The dynamic responses for the cylindrical shells, circular plates and conical shells using the two different techniques (wave approach and power series) can be coupled together by continuity of the displacements and slope and equilibrium of forces and moments at the cone/plate/cylinder junctions. The membrane forces ($N_x$, $N_\theta$, $N_{x\theta}$), bending moments ($M_x$, $M_\theta$, $M_{x\theta}$), transverse shearing $Q_x$ and the Kelvin–Kirchhoff shear force $V_x$ for the cylindrical shells, conical shells and circular plates are given in Ref. [14] per unit length. At the stern end cone/plate junction where the propeller force is applied, the eight continuity conditions are given by

$$u_c\cos\alpha-w_c\sin\alpha=w_p \tag{22}$$

$$w_c\cos\alpha+u_c\sin\alpha=u_p \tag{23}$$

$$v_c=v_p \tag{24}$$

$$-\frac{\partial w_c}{\partial x}=\frac{\partial w_p}{\partial r} \tag{25}$$

$$-(N_{x,c}\cos\alpha-V_{x,c}\sin\alpha)+N_{x,p}=F_0\varepsilon\cos(n\theta_0) \tag{26}$$

$$\left(N_{x\theta,c}+\frac{M_{x\theta,c}}{a}\right)+N_{\theta,p}=0 \tag{27}$$

$$M_{x,c}-M_{x,p}=0 \tag{28}$$

$$(V_{x,c}\cos\alpha+N_{x,c}\sin\alpha)+N_{r,p}=0 \tag{29}$$

Eqs. (22)–(25) are the continuity of displacement and slope, Eq. (26) is the continuity of the radial forces including the external excitation form the propeller and $\varepsilon=1/2\pi r_0$ if $n=0$ and $\varepsilon=1/\pi r_0$ if $n\neq 0$ as found by Eq. (21).

### 2.4.1. Inertial actuators

The control forces are generated using inertial actuators connected radially to the hull. Since the propeller force is applied to the stern of the hull, it is reasonable to locate the actuators on the prow end cone of the submarine. Inertial actuators are made of a mass $m_a$ suspended by a spring of stiffness $k_a$ and damping factor $c_a$. The electromagnetically generated force $f_a$ acts between the mass and the structure as shown in Fig. 4.

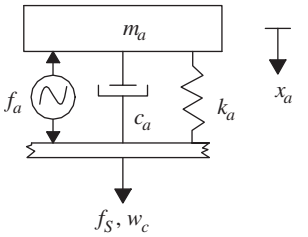


**Fig. 4.** Model of the inertial actuator.

The equation of motion for the mass of the actuator is given by

$$m_a\omega^2 x_a = f_a + k_a(x_a - w_c) - j\omega c_a(x_a - w_c) \tag{30}$$

$f_S$ is the force transmitted to the plate and it can be written as

$$f_S = T_a f_a + j\omega Z_a w_c \tag{31}$$

$$T_a = \frac{-\omega^2 m_a}{k_a - \omega^2 m_a - j\omega c_a}, \quad Z_a = \frac{-j\omega m_a k_a - \omega^2 m_a c_a}{k_a - \omega^2 m_a - j\omega c_a} \tag{32}$$

At frequency higher than the actuator resonance frequency $\omega_a = \sqrt{k_a/m_a}$ the mass provides a stable inertial platform to react the force [20]. The inertial actuators are positioned inside the prow end cone at $r=R_{ac}$ in order to form a circumferential array along the arc length $\sigma$ as shown in Fig. 5. Since only the bending modes have to be controlled, the inertial actuators forces amplitudes are spatially modulated in order to realise an excitation of the kind $f_S\cos(n\theta_c)$, with $n=1$ to excite only the bending modes as shown in Fig. 6. The conical shells were modelled as a junction of conical stripes joined together applying the boundary and continuity conditions [14]. The location of the actuators array is located at one of the aforementioned junctions. The continuity condition of the radial forces per unit length between two consecutive conical stripes reads

$$Q_{x,c+1} - Q_{x,c} = \delta_{n1}\frac{f_S}{2\pi R_{ac}}\cos(\theta_c) \tag{33}$$

where $\delta_{n1}$ is the Kronecker delta.

## 2.5. Steady-state response of the submarine

The steady-state response of the hull can be calculated as follows. For every circumferential mode number $n$ the boundary equations together with the equilibrium of the forces under point force excitation be arranged in the matrix form $\mathbf{A}_n\mathbf{u}_n = \mathbf{f}_n$, where $\mathbf{f}$ is the force vector containing the force $f_P$ from the propeller and/or $f_S$ from the active control actuators. Solving the system for each circumferential mode number gives the steady-state shell displacement response at a certain frequency. Defining the transfer function $\mathbf{H}_n = \mathbf{A}_n{}^{-1}$, the unknown coefficients of the plates and shells displacements can be obtained by $\mathbf{u}_n = \mathbf{H}_n\mathbf{f}_n$. As it was shown in Ref. [14], the structural and acoustic responses under a point radial excitation are dominated by only the $n=1$ (bending) modes. This allows the dynamics of both the axisymmetric modes and the higher order circumferential modes to be neglected since their effect is very small.

## 2.6. Active control

The harmonic excitation from the propeller is at the blade passing frequency (*bpf*). Since the primary force is tonal, a feedforward active control strategy is most appropriate [1]. Two kinds of active control strategies are investigated for the reduction of the noise radiated by the submarine: The Active Vibration Control (AVC) and the Active Structural Acoustic Control (ASAC). Aim of the AVC is to apply one or more secondary forces in order to reduce the structural vibrations excited

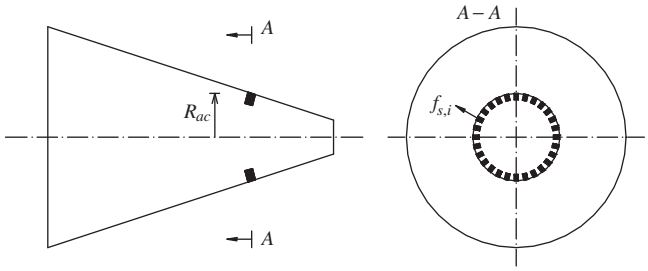


**Fig. 5.** Circumferential array of actuators on the end-plate.

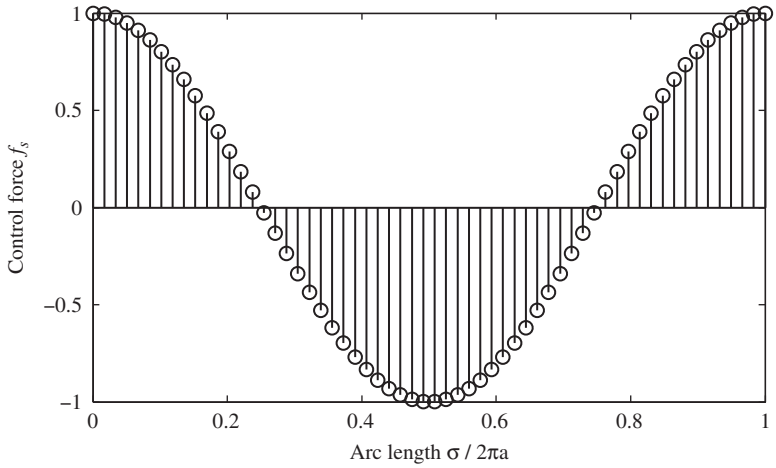


**Fig. 6.** Force distribution along the arc length.

by the primary force. The reduction of structural vibrations can eventually result in a reduction of the radiated noise. An error ($\mathbf{e}$) at one or more locations on the structure is defined as a sum of the axial displacement $\mathbf{u}_P$ resulting by the primary excitation plus the contribution from the secondary forces $\mathbf{f}_S$

$$\mathbf{e} = \mathbf{u}_P + \mathbf{u}_S, \quad \mathbf{u}_P = \mathbf{H}_P\mathbf{f}_P, \quad \mathbf{u}_S = \mathbf{H}_S\mathbf{f}_S \tag{34}$$

where $H_S$ is the transfer function between the secondary forces and the axial displacement. In case the number of error sensors excides or equates the number of control forces, the cost function to be minimised is defined as [1]

$$J = \mathbf{e}^H\mathbf{e} + \mathbf{f}_S^H\mathbf{R}\mathbf{f}_S \tag{35}$$

where the superscript $^H$ denotes the Hermitian of the vector and $\mathbf{R}$ is a Hermitian positive definite weighting matrix needed to reduce the values of the control forces to their physical limit and to evenly distribute the effort of the actuators. The optimum control force vector is given by [21]

$$\mathbf{f}_{S_o} = -(\mathbf{H}_S^H\mathbf{H}_S + \mathbf{R})^{-1}\mathbf{H}_S^H\mathbf{H}_P\mathbf{f}_P \tag{36}$$

The quadratic optimisation theory described for the AVC can also be applied for the Active Structural Acoustic Control where the goal is to attenuate the sound radiated in one or more directions. The radiated pressure is calculated by defining in the frequency domain, an acoustic transfer function $H_{u_ip_j}$ that maps the far-field sound pressure $p(R, \varphi_j)$ for $\theta$=0 to the displacement $w(x_0, \theta_0)$ as shown in Fig. 7 by

$$p(R,\phi_j) = H_{u_ip_j}w(x_0,\theta_0) \tag{37}$$

In this case the error can be written as

$$\mathbf{e} = \mathbf{p}_P + \mathbf{p}_S, \quad \mathbf{p}_P = \mathbf{H}_{up,P}\mathbf{H}_P\mathbf{f}_P, \quad \mathbf{p}_S = \mathbf{H}_{up,S}\mathbf{H}_S\mathbf{f}_S \tag{38}$$

This method allows the far field to be related to the sound pressure directly to the structural response. If the following assumptions are satisfied:

I. The primary force is measurable and its frequency can be changed.
II. The far-field pressure can be measured at least once.

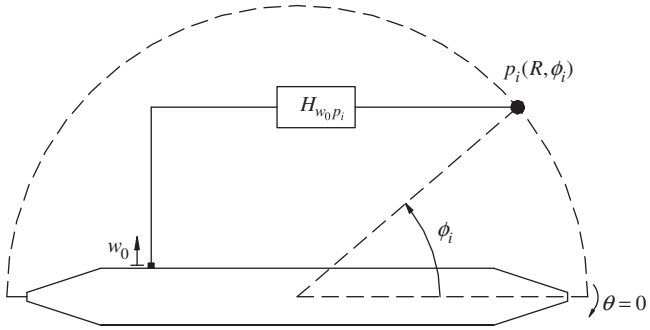


**Fig. 7.** Definition of the acoustic transfer functions by point measurement on the hull.

Then the following procedure can be applied:

- The structure is excited with a harmonic primary harmonic force varying the frequency or with an impulsive excitation.
- The radial displacement at location $x_0$ is measured and transformed in the frequency domain by Fourier transform.
- The sound pressure is measured at different locations $\theta_i$ in the far field and transformed in the frequency domain by Fourier transform.
- The transfer functions $H_{w_0 p_i}$ are calculated by $H_{u_0 p_i} = p(R,\phi_i)/w_0$.
- If assumptions I and II are not satisfied the calculation can be done using a numerical model.

The location of the structural sensor is chosen away from the regions affected by the near field vibrations, such as the structural junctions. For the location of the far-field pressure sensors, the nodes in the directivity patterns should also be avoided.

## 3. Sound radiated by the submarine hull

The sound radiated in the far field is calculated by solving the Helmholtz integral. The far field is defined in spherical coordinates ($R_r$, $\phi_r$, $\theta_r$) with the origin set at the geometric centre of the hull. The sound pressure is given by [14,22]

$$p_r(R_r,\phi_r,\theta_r) = \sum_{n=-\infty}^{\infty} p_{r,n}(R_r,\phi_r,n)e^{jn\theta_r} \tag{39}$$

where

$$p_{r,n}(R_r,\phi_r,n) = (-j)^{|n|}\frac{e^{jk_f R_r}}{2R_r}\frac{1}{\omega\rho_f c_f}\int_{z_1}^{z_m} Y(r_0,n,z_0)e^{-j\alpha z_0}\frac{r_0}{\cos\beta}\,dz_0 \tag{40}$$

$$Y(r_0,n,z_0) = p_0(r_0,n,z_0)[\gamma\cos\beta J'_{|n|}(\gamma r_0) + j\alpha_r \sin\beta J_{|n|}(\gamma r_0)] - \rho_f\omega^2 W(r_0,n,z_0)J_{|n|}(\gamma r_0) \tag{41}$$

The axisymmetric surface of the hull is represented by Cartesian coordinates ($r$, $z_r$), where $z_r$ is in the axial direction with its origin set at the geometric centre of the hull. $a_r$ is the radius of the structure at location $z_r$. The surface $S_0$ extends from $z_1$ to $z_m$. ($r_0$, $z_0$) is the node location on the hull surface $S_0$. $\alpha_r = k_f\cos\theta_r$, $\gamma = k_f\sin\theta_r$ and $\beta$=atan($\partial a_r(z_r)/\partial z_r$). Once the radial displacement $W(r_0, z_0)$ at each node ($r_0$, $z_0$) on the boundary of the structure has been evaluated, as described in the previous section, the shell surface pressure $p_0(r_0, z_0)$ at each node on the shell surface can be then calculated by $\mathbf{p}_0 = \mathbf{D}\mathbf{w}_0$, where $\mathbf{D}$ is the fluid matrix and $\mathbf{p}_0$, $\mathbf{w}_0$ are the vectors of the surface pressure and radial displacement, respectively [14].

## 4. Numerical results

Numerical results are presented for a submarine hull made of a cylindrical shell of radius $a$=3.25 m, thickness $h$=0.04 m, length $L$=45 m and with T-ring stiffeners evenly spaced by $b$=0.5 m. A distributed mass on the shell of $m_{eq}$=1500 kg m$^{-2}$ was used. The hull has two evenly spaced bulkheads of thickness $h_p$=0.04. The cylindrical hull is closed by truncated conical end caps with semi-vertex angle of $\alpha$=18°, thickness $h_c$=0.014 m and smaller radius of $R_1$=0.50 m. The thickness of the end-plates is the same as for the bulkheads. All the structures are made of steel with density $\rho$=7800 kg m$^{-3}$, Young's modulus $E$=2.1 × 10$^{11}$ N m$^{-2}$ and Poisson's ratio $\upsilon$=0.3. Structural damping was introduced using a complex Young modulus $E(1-j\eta)$, where $\eta$=0.02 is the structural loss factor.

Results are presented considering a unitary harmonic force from the propeller in the frequency range 0–80 Hz. The typical *bpf* for a large submarine at maximum speed is around 25 Hz. Higher values of frequency contain the super harmonics which have much smaller amplitude [19]. The results should be scaled in case real data of the excitation are

available. An array of 60 actuators is positioned inside the prow end cone with a radius of $R_{ac}$=1.0 m. The inertial actuators are taken by a commercially available model and have the following data: suspended mass $m_a$=2.2 kg, spring stiffness $k_a$=6130 N m$^{-1}$, damping factor $c_a$=34.8 N m$^{-1}$ s, damping factor $c_a$=34.8 N m$^{-1}$ s and diameter $\phi$=90 mm. The control strategies reported in Table 1 are investigated. For ASAC, the pressure at the error locations is estimated by a transfer function with a point measurement on the cylindrical shell at $x$=2 m.

Fig. 8 shows the frequency response function (FRF) at the error sensor location $x$=2 m. Using (AVC 1e) the response is negligible as expected. The radial displacement result from applying the ASAC is less affected by the control since the goal is to minimise the sound radiated.

Fig. 9 shows the sound power level with and without active control. It can be seen that the best results are given by ASAC with eight error sensors. The reduction at resonances is very good at low frequencies. Lack of performance is observed at high frequencies and out of resonance, probably due to the high modal density of the bending modes. At around 60 Hz the cutting-on of the second class of waves [14] is observed and the active control is ineffective. Reduction of the structural vibration, given by (AVC 3e), results in reduction of radiated power in some frequency ranges but not with results as good as in the case of ASAC. Furthermore minimising the radial response only at one error sensor (AVC 1e) leads

**Table 1**
Active control strategies investigated.

| Control | Location of error sensors |
|---|---|
| ASAC 8e | $\theta$=[0, 15, 30, 75, $q$=105, 150, 165, 180]°<br>$\phi$=0° |
| AVC 1e | $x$=2 m |
| AVC 3e | $x$=[2, 22.5, 43] m |

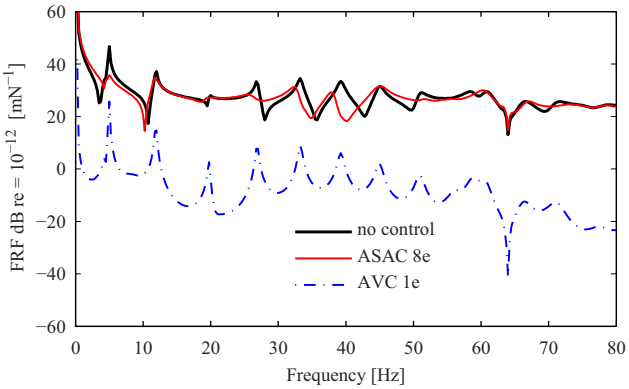


**Fig. 8.** Frequency response function of the cylinder radial displacement at $x$=2 m.

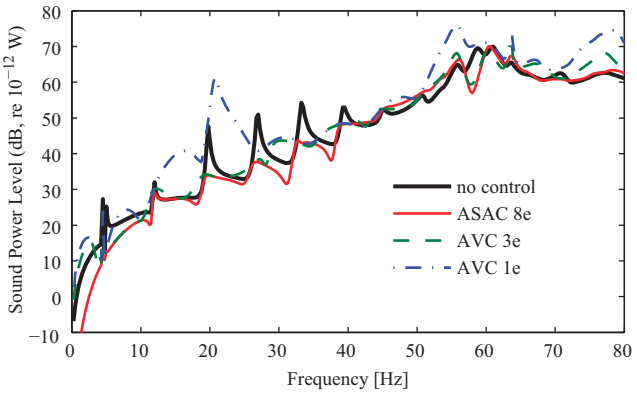


**Fig. 9.** Sound power level with and without control.

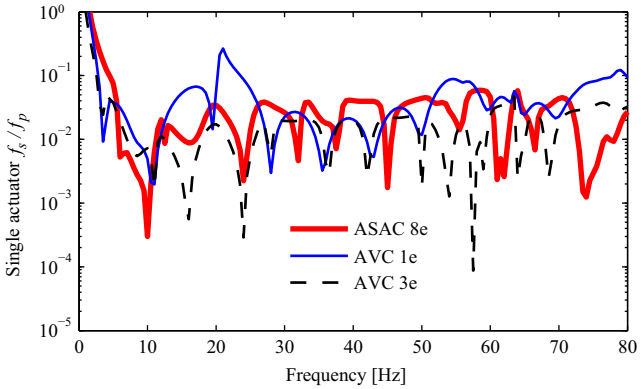


**Fig. 10.** Active optimum control forces for a single actuator.

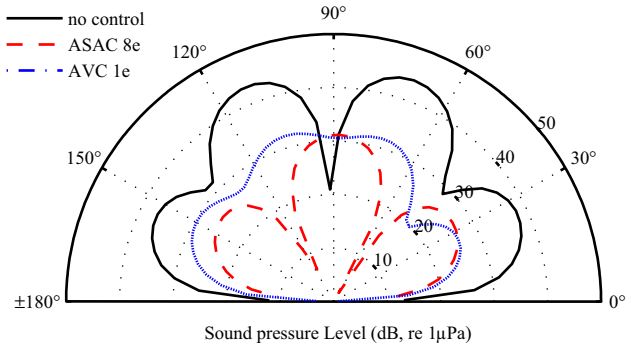


**Fig. 11.** Directivity pattern at *bpf*=27 Hz.

to an increase of radiated sound in the whole frequency range investigated. The reason is that the aim of AVC is to reduce the structural response and not the radiated sound.

Fig. 10 shows the control forces divided by the propeller force for a single inertial actuator of the arrays for ASAC and AVC. The ratio of control forces over the propeller amplitude are below the unity but to estimate the performances in a real vessel, the actual propeller force and the actuators' physical limits should be taken into account. A typical blade passing frequency for a submarine at its maximum speed is around 25 Hz and the amplitude of the fluctuating force can be estimated in around 2000 N. The closest resonance of the hull is at around 27 Hz where the control force for a single actuator using (ASAC 8e) have a magnitude of $f_s$=75 N, value achievable by the inertial actuators. At very low frequency the active control is not practical.

The directivity pattern at 27 Hz, where the resonance of the fourth bending mode is located, is shown in Fig. 11 and very good attenuation is observed with ASAC 8e and AVC 1e.

## 5. Conclusions

Active control strategies such AVC and ASAC have been investigated to reduce the sound radiated by a submarine hull under radial excitation from the propeller. A model of submarine was presented coupling cylindrical shells, conical shells and circular plates. The submerged vessel was excited by a harmonic force from the propeller. Inertial actuators were arranged in circumferential arrays and located at the prow end cone. An acoustic transfer function was defined in order to estimate the radiated sound by a single point measurement on the structure. It was shown that inertial actuators can deliver enough force to reduce the sound pressure in the far field and very good attenuation is observed at the resonant frequencies at low frequency. The aim of this work is to suggest that inertial actuators could be used to reduce the sound radiated by a submerged vessel in bending vibration. To verify the real performance of the active control, the actual design and the real magnitude and spectrum of the fluctuating forces form the propeller should be taken into account. In this work, a single array of actuators was considered but the application of active control can be extended using several arrays located inside the cylindrical or the conical shells.

## References


[1] C.R. Fuller, S.J. Elliott, P.A. Nelson, *Active Control of Vibration*, Academic Press, London, 1996.
[2] D. Ross, *Mechanics of Underwater Sound*, Pergamon, New York, 1976.
[3] P.G. Dylejko, Optimum Resonance Changer for Submerged Vessel Signature Reduction, PhD Thesis, The University of New South Wales, Sydney, Australia, 2007.
[4] A.J.H. Goodwin, The design of a resonance changer to overcome excessive axial vibration of propeller shafting, *Transactions of the Institute of Marine Engineers* 72 (1960) 37–63.
[5] C.P. Rigby, Longitudinal vibration of marine propeller shafting, *Transactions of the Institute of Marine Engineers* 60 (1948) 67–78.
[6] H. Schwanecke, Investigations on the hydrodynamic stiffness and damping of thrust bearings in ships, *Transactions of the Institute of Marine Engineers* 91 (1979) 68–77.
[7] X. Pan, Y. Tso, R. Juniper, Active control of radiated pressure of a submarine hull, *Journal of Sound and Vibration* 311 (2008) 224–242.
[8] X. Pan, Y. Tso, R. Juniper, Active control of low-frequency hull-radiated noise, *Journal of Sound and Vibration* 313 (2008) 29–45.
[9] W.T. Baumann, W.R. Saunders, H.H. Robertshaw, Active suppression of acoustic radiation from impulsively excited structures, *Journal of the Acoustical Society of America* 90 (1991) 3202–3208.
[10] Y. Gu, R.L. Clark, C.R. Fuller, A.C. Zander, Experiments on active control of plate vibration using piezoelectric actuators and polyvinylidene (PVDF) modal sensors, *Journal of Vibration and Acoustics—Transactions of the ASME* 116 (1994) 303–308.
[11] C.K. Lee, F.C. Moon, Modal sensors/actuators, *Journal of Applied Mechanics* 57 (1990) 434–441.
[12] J.P. Maillard, C.R. Fuller, Active control of sound radiation from cylinders with piezoelectric actuators and structural acoustic sensing, *Journal of Sound and Vibration* 222 (1999) 363–388.
[13] J.P. Maillard, C.R. Fuller, Advanced time domain wave-number sensing for structural acoustic systems. I. Theory and design, *Journal of the Acoustical Society of America* 95 (1994) 3252–3261.
[14] M. Caresta, N.J. Kessissoglou, Acoustic signature of a submarine hull under harmonic excitation, *Applied Acoustics* 71 (2010) 17–31.
[15] A. Rosen, J. Singer, Vibrations of axially loaded stiffened cylindrical shells, *Journal of Sound and Vibration* 34 (1974) 357–378.
[16] M. Caresta, N.J. Kessissoglou, Free vibrational characteristics of isotropic coupled cylindrical-conical shells, *Journal of Sound and Vibration* 329 (2010) 733–751.
[17] A.W. Leissa, *Vibration of Plates*, American Institute of Physics, New York, 1993.
[18] M. Abramowitz, I.A. Stegun, *Handbook of Mathematical Functions with Formulas, Graphs, and Mathematical Tables*, Dover Publications, New York, 1972.
[19] J.P. Breslin, P. Andersen, *Hydrodynamics of Ship Propellers*, Cambridge University Press, 1994.
[20] L. Benassi, S.J. Elliott, P. Gardonio, Active vibration isolation using an inertial actuator with local force feedback control, *Journal of Sound and Vibration* 276 (2004) 157–179.
[21] P.A. Nelson, S.J. Elliott, *Active Control of Sound*, Academic Press, London, 1992.
[22] E.A. Skelton, J.H. James, *Theoretical Acoustics of Underwater Structures*, Imperial College Press, London, 1997.